Ocular Dominance Column Development: Analysis and Simulation

KENNETH D. MILLER, JOSEPH B. KELLER, MICHAEL P. STRYKER

The visual cortex of many adult mammals has patches of cells that receive inputs driven by the right eye alternating with patches that receive inputs driven by the left eye. These ocular dominance patches (or "columns") form during early life as a consequence of competition between the activity patterns of the two eyes. A mathematical model of several biological mechanisms that can account for this development is presented. Analysis of this model reveals the conditions under which ocular dominance segregation will occur and determines the resulting patch width. Simulations of the model also exhibit other phenomena associated with early visual development, such as topographic refinement of cortical receptive fields, the confinement of input cell connections to patches, monocular deprivation plasticity including a critical period, and the effect of artificially induced strabismus. The model can be used to predict the results of proposed experiments and to discriminate among various mechanisms of plasticity.

IN THE VISUAL SYSTEMS OF MANY MAMMALS, INCLUDING CATS, monkeys, and humans, the optic nerves from the two eyes project to separate layers of a relay nucleus, the lateral geniculate nucleus (LGN) of the thalamus. Fibers from the LGN in turn project to cortical layer 4, the input layer of the primary visual cortex. There they terminate in alternate patches called "ocular dominance columns" serving the left eye and right eye, respectively (Fig. 1). The nonoverlapping pattern of connections evolves during development. Initially the connections representing the two eyes are distributed throughout layer 4, overlapping completely. Subsequently, they become segregated into two sets of patches, one for each eye.

Ocular dominance patch formation appears to depend on competition between the activity patterns originating within the two eyes (*1*). The patches do not develop when neural activity is blocked in the eyes or in the cortex or when a pattern of neural activity is given synchronously to the nerves from both eyes. They do develop when the activity patterns in the nerves from the two eyes are asynchronous. Closing one eye during a critical period early in development (monocular deprivation) results in larger patches for the open eye and smaller patches for the closed eye. Closing of both eyes during the same period causes no abnormal effect. Thus, both development of ocular dominance patches and the effects of monocular deprivation involve competition between activity patterns; they do not result simply from the presence or absence of activity.

This competition provides a model system for understanding activity-dependent synaptic plasticity. We presume that the strengthening of some synapses and the weakening of others are governed by cellular-level rules involving the patterns of neural activity onto and by each cortical cell. These small-scale changes, occurring on many individual cells during development, result in the large-scale structure of ocular dominance.

Various cellular-level mechanisms for plasticity have been proposed (*2*). Simulations by von der Malsburg and others (*3*) have demonstrated that some of these mechanisms can produce ocular dominance patches. We have developed a mathematical model that describes several such mechanisms. From it, we can determine the ocular dominance structure that would result from each mechanism, given experimental values for biological parameters (*4*).

Our analysis focuses on four biological features that are thought to play a role in organizing ocular dominance patches (Fig. 2):

1) The patterns of initial connectivity of the geniculocortical afferents (inputs from geniculate to visual cortex) onto the cortical cells. These patterns involve the spread of afferent arbors and of cortical dendrites and are described by an "arbor function," A.

2) The patterns of activity in the afferents. These patterns are described by a set of four "correlation functions," C^{LL}, C^{RR}, C^{LR}, and C^{RL}. They describe correlations in activity between afferents serving the same eye, left or right (C^{LL} and C^{RR}) or serving different eyes (C^{LR} and C^{RL}).

3) Influences acting laterally within the cortex, whereby synapses on one cell can influence the competition occurring on nearby cells.

K. D. Miller is in the Department of Physiology, University of California, San Francisco, CA 94143–0444, where he has worked while a graduate student in the Department of Neurobiology, Stanford University, Stanford, CA 94305. The work presented here forms part of his Stanford Ph.D. dissertation. J. B. Keller is a member of the Department of Mathematics, Stanford University, Stanford, CA 94305. M. P. Stryker is a member of the Department of Physiology and Neuroscience Graduate Program, University of California, San Francisco, CA 94143–0444.

These influences, described by a "cortical interaction function," I, may occur through corticocortical synaptic connections or diffusion of modulatory substances.

4) Constraints limiting the total synaptic strength supported by an afferent or cortical cell.

The sizes of some of these features have been measured in the visual cortex of adult cats. The final patches have periodicity of about 850 μm (*5, 6*). Initial arbors may fill a region with diameter 1 to 1.5 mm (X cells) or larger than 2 mm (Y cells) (*7*). Afferents from a single eye appear positively correlated in darkness over distances of from 1/2 (for X cells) to 3/2 (for Y cells) of a geniculocortical arbor radius (*8*). Corticocortical synaptic interactions may be excitatory at short range and are inhibitory at further distances to about 400 μm; longer range, periodic cortical connections also exist (*9*). Most of these features have not yet been measured in kittens, when columns are developing.

The purpose of this analysis is to demonstrate the role of each of these four features in ocular dominance segregation. The model shows that ocular dominance patches emerge from an initially uniform state when the state is unstable to small perturbations. The model also describes the development of structure within individual cortical receptive fields and geniculate axon terminal arborizations ("arbors"). We shall characterize the general conditions on the four features under which a pattern-forming instability exists and determine the width of the ocular dominance patches that emerge. The results predict the patterns of ocular dominance organization that should result under various experimental conditions and thereby permit discrimination among proposed mechanisms of plasticity.

Formulation of the Equations

We model layer 4 of the cortex and two geniculate laminae, each serving one eye, as three two-dimensional sheets. Consider afferents serving the left eye with cell body at position α in the LGN (Fig. 2) (*10*). Suppose the terminal arborizations of these cells make synaptic contact with cortical cells at the position x. We denote the number of such synapses by the arbor function $A(x - \alpha)$ and their total synaptic strength at time t by $S^L(x,\alpha,t)$. Similarly, $S^R(x,\alpha,t)$ denotes the corresponding strength for the right eye. $A(x - \alpha)$ is taken to be a decreasing function of the retinotopic distance between geniculate and cortical cells and is the same for both eyes.

We begin by formulating an equation for Hebbian synapses, which are strengthened when presynaptic activity is sufficiently correlated with activation of the postsynaptic cell and weakened otherwise (*11*). This equation can be written for individual synapses as $\Delta s = [(post)(pre) - (decay)]\Delta t$, where Δs is the change in the synaptic strength in a small time interval Δt, and *post* and *pre* are functions of postsynaptic and presynaptic activities, respectively.

We assume that cortical activity is determined by the combined activity of all the afferents from the LGN to the cortex. Then *post* can be replaced by a function of presynaptic activities and of synaptic strengths. We then obtain the following equation governing $S^L(x,\alpha,t)$ (*12–15*):

$$\frac{dS^L(x,\alpha,t)}{dt} = \lambda A(x - \alpha)\sum_{\gamma,\beta} I(x - \gamma)[C^{LL}(\alpha - \beta)S^L(\gamma,\beta,t) + C^{LR}(\alpha - \beta)S^R(\gamma,\beta,t)] - \gamma S^L(x,\alpha,t) - \varepsilon A(x - \alpha) \quad (1)$$

Interchanging L and R yields the equation for S^R. Similar equations have been derived by a number of investigators (*16–21*).

In Eq. 1, $C^{LL}(\alpha - \beta)$ is a measure of the correlation between the activities of the left-eye afferents from points α and β in the LGN. $C^{LR}(\alpha - \beta)$ is the corresponding correlation measure for left-eye afferents from α and right-eye afferents from β. The cortical interaction function $I(x - \gamma)$ describes the total influence on the cortical cell at x of geniculate excitation of the cortical cell at γ. This includes direct excitation, if $\gamma = x$, and indirect effects via excitation of intermediate cortical cells that may excite or inhibit the cell at x.

Equation 1 for S^L and the corresponding equation for S^R constitute our basic mathematical model of synaptic strength development. The data used in the model are the arbor function $A(x - \alpha)$, the cortical interaction function $I(x - \gamma)$, and the correlation functions such as $C^{LL}(\alpha - \beta)$. When the initial values of S^L and S^R are given at time $t = 0$, the equations determine S^L and S^R at any later time t.

This basic model must be modified to prevent synaptic strength from becoming negative or from becoming too large. Nonlinearities must be included in the equation to enforce these conditions. In addition, the model may be modified to limit the total synaptic strength supported by a cortical or afferent cell (*22*). Terms must be added to the equations to enforce such limits.

We have investigated Eq. 1, subject to these conditions, by using computer simulations and analytical methods to determine the conditions on the functions A, I, and C under which column development and other features of visual cortical development occur. We choose a particular model for the conditions limiting synaptic strengths in the simulations and explore the role of these conditions more generally in the analysis.

Simulations

We represent layer 4 of the cortex and two LGN laminae, one representing each eye, as three 25 × 25 grids of cells. Periodic boundary conditions are used, so that the topmost and bottommost

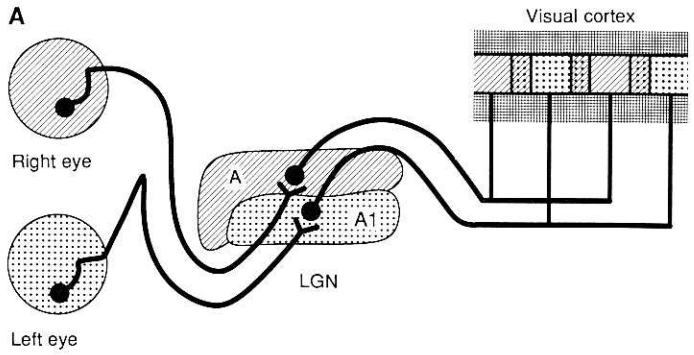

Fig. 1. (**A**) Schematic of the visual system after development of ocular dominance patches. The left lateral geniculate nucleus (LGN) and visual cortex are pictured. Retinal ganglion cells from the two eyes project to separate laminae of the LGN. The right (contralateral) eye projects to lamina A, and the left (ipsilateral) eye projects to lamina A1. Neurons from these two layers in turn project to separate patches or stripes within layer 4 of the primary visual cortex. The cortex is depicted in cross section, so that layers 1 through 3 are above and layers 5 and 6 are below the layer 4 projection region. Binocular regions are pictured at the borders between patches in layer 4. (**B**) Ocular dominance patches in layer 4 of the cat visual cortex. Photomontage was constructed from tangential sections taken through layer 4 of flattened cortex. Geniculocortical afferent terminals representing the ipsilateral eye were labeled and appear white. [From figure 6D of (*6*), with permission of the *Journal of Neuroscience*]

rows within each grid are regarded as neighbors, as are the leftmost and rightmost columns within each grid. Each LGN cell arborizes to contact a 7×7 square of cortical cells centered on its retinotopic position in the cortex. Thus there are $2 \times (25 \times 25) \times (7 \times 7) = 61{,}250$ synapses. Initially the strength of each synapse is assigned a value chosen randomly from a distribution uniform between 0.8 and 1.2. We limit synaptic strengths to a range between 0 and 8.0 and impose constraints fixing the total synaptic strength supported by a cortical cell and limiting or fixing the total synaptic strength over an afferent arbor. We solve Eq. 1 beginning from the random initial conditions and subject to these limits and constraints (*23*).

Figure 3 shows typical development under the model. Initially the cortex is binocular everywhere with approximately equal input from the two eyes, indicated by the color blue in Fig. 3A. Gradually, synapses driven by the right and left eyes segregate, indicated by red and green, respectively, dividing the cortical territory into ocular dominance patches. Biologically, the development of ocular dominance patches is accompanied by (i) development of monocular receptive fields of cortical neurons, (ii) topographic refinement of receptive fields, and (iii) the progressive confinement of individual LGN axon arbors to patches. We examine the set of LGN inputs to a cortical cell as representative of the cell's receptive field. Figure 3B shows the development of eight such sets. Initially, each cortical cell has synapses of uniform strength from both eyes throughout the field. The inputs from each eye become concentrated in the centers of each receptive field, producing topographic refinement. Subsequently, the cells become monocular, that is, one eye gives strong input (red) and the other eye's input is lost (gray). Geniculate afferent arbors (Fig. 3C) also are initially uniform and then concentrate their strength centrally. Subsequently, the two axonal arbors from the two eyes stemming from a single retinotopic position in the LGN segregate into complementary regions. These regions correspond to the cortical patches.

These results are completely robust, because qualitatively identical results were obtained for every set of random initial conditions tried. Figure 4 shows the final cortical layer 4 patterns of ocular dominance resulting from four different random initial conditions. Although the precise locations of the patches vary from trial to trial, the qualitative and essential quantitative nature of the patches remains invariant.

The precise afferent correlations, cortical interactions, and spread of afferent connections in kittens are not yet known. Furthermore, these functions will vary among species and under experimental perturbations. Therefore, it is important to determine how the developmental outcome depends on these functions. To do so, we simulated development with each of various correlation functions, cortical interaction functions, and arbor functions. In the results presented below, the initial conditions and all functions except the one being studied remain identical to those used in Fig. 3. These results confirm and supplement more general results obtained analytically, which will be discussed subsequently.

We studied development with correlation functions varied in several systematic ways (Fig. 5A). First, we considered a broader or narrower Gaussian correlation function within each eye, with zero correlation between the two eyes (labeled "same-eye correlations" in Fig. 5A). As shown in Fig. 6A, the broader the range of correlations, the more purely monocular the resulting cortex. The cortex resulting from broader correlations resembles that of the monkey in having few binocular cells at the borders of patches (*24*), whereas that resulting from narrower correlations resembles that of the cat in having many binocular cells at the patch borders (*25, 26*). On the basis of these results and results obtained with correlation functions that are constant over some finite range, we conclude that correlation among nearest neighbors (adjacent grid points) is sufficient to give a periodic pattern of ocular dominance, whereas positive correlation over an arbor radius (± 3 grid points) seems sufficient to achieve a fully monocular cortical layer 4.

Second, anticorrelations were added to such a function, either between afferents of the two different eyes (labeled "+opp-eye anticorr") or between distantly spaced afferents within a single eye (labeled "+same-eye anticorr"). Addition of opposite-eye anticorrelations can be taken to model strabismus or alternating monocular deprivation, treatments that increase the monocularity of cortex, or to reflect a possible feature of normal LGN circuitry (*27*). Addition of opposite-eye anticorrelations increases the monocularity of the simulated layer 4, as in experiments. In contrast, addition of anticorrelations within each eye decreases monocularity. If present within an arbor radius, such anticorrelation largely destroys monocularity (same-eye anticorr 1.4, Fig. 6A).

An alternative type of cortical interaction function that is purely excitatory is shown in Fig. 5B. With this interaction, one eye tends to dominate most or all of cortex. However, if the total synaptic strength supported by each arbor is fixed, the two eyes must remain equal in their total synaptic strength. The result is that a pattern of ocular dominance patches forms, with the width of left-eye plus right-eye patches slightly larger than before and approximately equal to an arbor diameter (Fig. 6B). Thus, periodic segregation of ocular dominance can occur in the absence of lateral inhibition.

The arbor function was modified to decrease with distance over the 7×7 range of connection. This represents decreasing connectivity. The result (not shown) is to decrease the period of the ocular dominance patches and to reduce the sizes of the final receptive fields and arbors.

The model thus reproduces many features of normal development for a wide range of correlations, cortical interactions, and arbors. The degree of monocularity of the final cortex depends on afferent correlations, whereas the widths of the patches can be altered by varying the intracortical interactions or the arbor function.

We studied monocular deprivation, modeling it as a reduction in the amount of activity in the deprivied eye without alteration of the correlational structure of that activity. This corresponds to a reduction in the amplitude of the correlation function within that eye. Disruption of the correlations would only increase the effects of deprivation. The result of deprivation, both in the model and experimentally, is that the normal eye takes over more than its normal share of the cortex (Fig. 7). There is a critical period for this effect in the model, as is seen biologically; that is, the effect of deprivation is progressively weaker for later onset.

The critical period in the model has two causes. One cause is strictly dynamical, requiring neither changes in plasticity rules nor stabilization of synapses. Once the cortex has a sufficient degree of ocular dominance organization, the deprived eye's greater synaptic strength, within its dominance domains, more than compensates for its weaker activity. In these domains the deprived eye therefore remains stable against competition from the normal eye. However, cells that remain binocular remain susceptible to domination by the more active eye. Binocular cells will become resistant to such domination if individual synapses are stabilized (rendered no longer modifiable) when they reach a saturating strength. Hence, stabilization of saturated synapses is the second cause of the critical period in the model. The dynamical mechanism is sufficient to completely account for the critical period when, as in Fig. 7, cells in layer 4 become fully monocular in the absence of deprivation. If, as in the cat, many cells in layer 4 normally remain binocular, the dynamical mechanism can nonetheless contribute to the critical period by ensuring that regions that become sufficiently dominated by one eye are no longer subject to an ocular dominance shift.

When cortical cells, but not afferents, are pharmacologically

inhibited during monocular deprivation, the experimental result is a shift in responsiveness in favor of the closed eye (*28*). To model this, we note that *post* in the Hebbian equation $\Delta s = [(post)(pre) - (decay)]\Delta t$ becomes equal to a negative constant, because all cortical cells are inhibited [see Eq. 3 in (*15*)]. Then there is no coupling between synapses; each synapse decays in proportion to *pre*, which is a measure of its presynaptic activity. This "punishes" the more active synapses and, given constraints to preserve total synaptic strength over a cell, favors the afferents from the less active eye as in experiment.

Analysis

The simulations demonstrate that both normal and experimentally perturbed development of ocular dominance columns are reproduced by the model. These results can largely be explained by the following intuitive analysis. First, consider geniculate synapses onto a single cortical cell in the absence of interactions with synapses on other cortical cells. Each synapse then grows in proportion to the sum of its correlations with all other synapses on the cell, weighted by the strengths of those synapses. Receptive fields refine topographically, because synapses representing the center of the receptive field are strongly correlated with larger numbers of synapses than are synapses representing the periphery. This causes the central synapses to grow more rapidly than the peripheral ones. Similarly, receptive fields become monocular, because synapses serving each eye are better correlated with other synapses serving the same eye. This causes synapses of the eye with an initial advantage in overall synaptic strength to grow faster. Because this initial advantage is very slight compared to the advantage of central over peripheral synapses, monocularity develops more slowly than receptive field refinement.

Broader correlations within each eye enhance the growth of a monocular pattern of inputs compared to that of a binocular pattern and thus enhance monocularity. Broader correlations also reduce the advantage of central synapses over peripheral ones. Anticorrelations between the two eyes enhance the difference in growth rate between synapses of the two eyes and hence also enhance development of monocularity. Same-eye anticorrelations within an arbor radius cause a synapse's growth to be reduced by the presence of synapses of the same eye in an adjacent part of the receptive field. This causes binocular cells to develop, because a binocular pattern of inputs then grows more quickly than a monocular one. Thus, the development of monocularity and of receptive field refinement can be understood from the correlation functions.

Now consider the effects of intracortical interactions on the growth of a monocular set of inputs to one cortical cell. The set's growth is most enhanced if inputs to surrounding cortical cells fire in correlation over distances at which intracortical interactions are excitatory, and fire without correlation over distances at which intracortical interactions are inhibitory. Hence, the monocular inputs grow fastest if surrounded by a "bull's eye" of inputs from the same eye at excitatory distances and of inputs from the opposite eye at inhibitory distances. Although each monocularly driven cortical cell cannot be at the center of its own bull's eye, a compromise can be reached through a periodic organization such as patches or stripes. The period of this organization is like that of the bull's eye and is determined by the intracortical interactions.

To gain a more precise understanding of the roles played by afferent correlations, arbors, and cortical interactions in causing ocular dominance segregation and in determining patch widths, we analyze the equations mathematically. To do so, we assume that the two eyes are equivalent in their activities and their initial projections. Thus we ignore the effects of slight (5 to 10%) overall bias toward the contralateral eye in the cat (*26*) and we restrict our analysis to exclude monocular deprivation. Equivalence of the eyes implies $C^{LL} = C^{RR}$, $C^{LR} = C^{RL}$. Subtracting Eq. 3 for S^L from Eq. 3 for S^R yields an equation for the time evolution of the difference, $S^D \equiv S^R - S^L$, between the synaptic strengths of the two eyes at a given location in the cortex:

$$\frac{dS^D(x,\alpha,t)}{dt} = \lambda A(x-\alpha)\sum_{\beta,\gamma} I(x-\gamma)C^D(\alpha-\beta)S^D(\gamma,\beta,t) - \gamma S^D(x,\alpha,t) \quad (2)$$

Here $C^D \equiv C^{LL} - C^{LR}$. The function $C^D(\alpha - \beta)$ measures the extent to which afferents at geniculate locations α and β are more correlated if they are from the same eye than if they are from opposite eyes.

Initially the difference in synaptic strengths, S^D, is very close to zero. We examine the stability of the state $S^D \equiv 0$ by examining whether a small initial perturbation of this state will grow or decay. Growth will result in a pattern of ocular dominance, whereas decay will yield a state of complete equality of the two eyes. If $S^D \equiv 0$ is unstable, many geniculocortical patterns of S^D may grow from the initial perturbation. The fastest growing such pattern will quickly dominate. Its characteristic periodicity will determine the width of the patches or stripes. The initial pattern-forming instability occurs when S^D is small, so only linear terms in an equation for S^D are relevant to this analysis. Thus the results will be robust to nonlinearities such as those inherent in biological development (*29*).

The Characteristic Patterns of Ocular Dominance

We refer to the patterns that grow exponentially, from a perturbation of $S^D \equiv 0$, as characteristic patterns of ocular dominance. Technically, these are the eigenfunctions of the operator in Eq. 2.

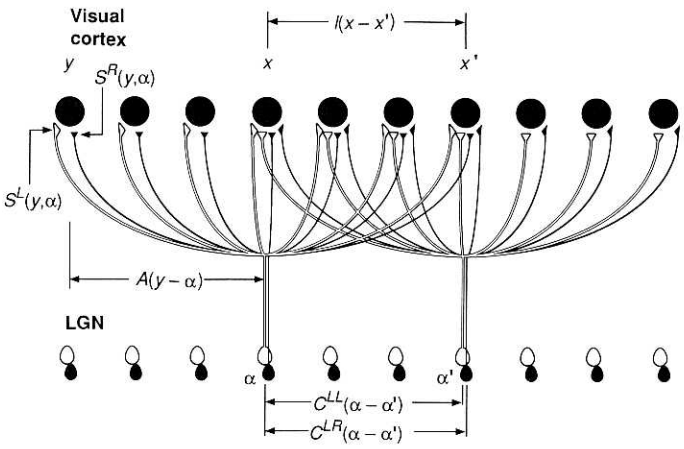

Fig. 2. Notation. Afferents from left-eye (white) and right-eye (black) layers of the LGN innervate layer 4 of the visual cortex. α and α' label positions in the LGN, and x and x' label the retinotopically corresponding points in the cortex; y labels an additional position in the cortex. The afferent correlation functions C^{LL} (correlation in activity between two left-eye afferents) and C^{LR} (correlation in activity between a left-eye and a right-eye afferent) are functions of separation across the LGN. The arbor function A measures anatomical connectivity (number of synapses) from a geniculate point to a cortical point, as a function of the retinotopic distance between them. The cortical interaction function I depends on a distance across cortex. The left-eye and right-eye synaptic strengths, S^L and S^R, from a geniculate location to a cortical location, depend upon both locations.

Each characteristic pattern of ocular dominance is of a form similar to $S^D(x,\alpha) = \cos k \cdot x\ R(x - \alpha)$ (*30*). Figure 8 shows the fastest growing such pattern for the functions used in the simulation of Fig. 3. The factor $R(x - \alpha)$ represents a characteristic receptive field. This is the pattern of differences between left- and right-eye synaptic strengths in the input to a cortical cell. Where it is positive one eye is dominant, and where it is negative the opposite eye is dominant. A monocular characteristic receptive field, like that of Fig. 8, is one dominated by a single eye throughout, so that R can be taken positive everywhere. Characteristic receptive fields need not be monocular: they may show division of the receptive field into domains dominated by opposite eyes.

The factor $\cos k \cdot x$ represents an oscillation in the degree of dominance of receptive fields across the cortex. In Fig. 8, the leftmost receptive field occurs at a cortical point x where $\cos k \cdot x = 1$, so the right eye is dominant. The central receptive field occurs at a point x' where $\cos k \cdot x' = 0$, so the two eyes are equal. The rightmost receptive field occurs at a point x'' where $\cos k \cdot x'' = -1$, so the left eye is dominant. In the case of monocular characteristic fields, it is this oscillation, between ocular dominance by one eye and by the other, that causes organization of monocular cortical cells into ocular dominance patches. We refer to the spatial period or wavelength of this oscillation as the wavelength of the characteristic pattern. This wavelength corresponds to the width of left-eye patch plus right-eye patch, which we refer to simply as the patch width.

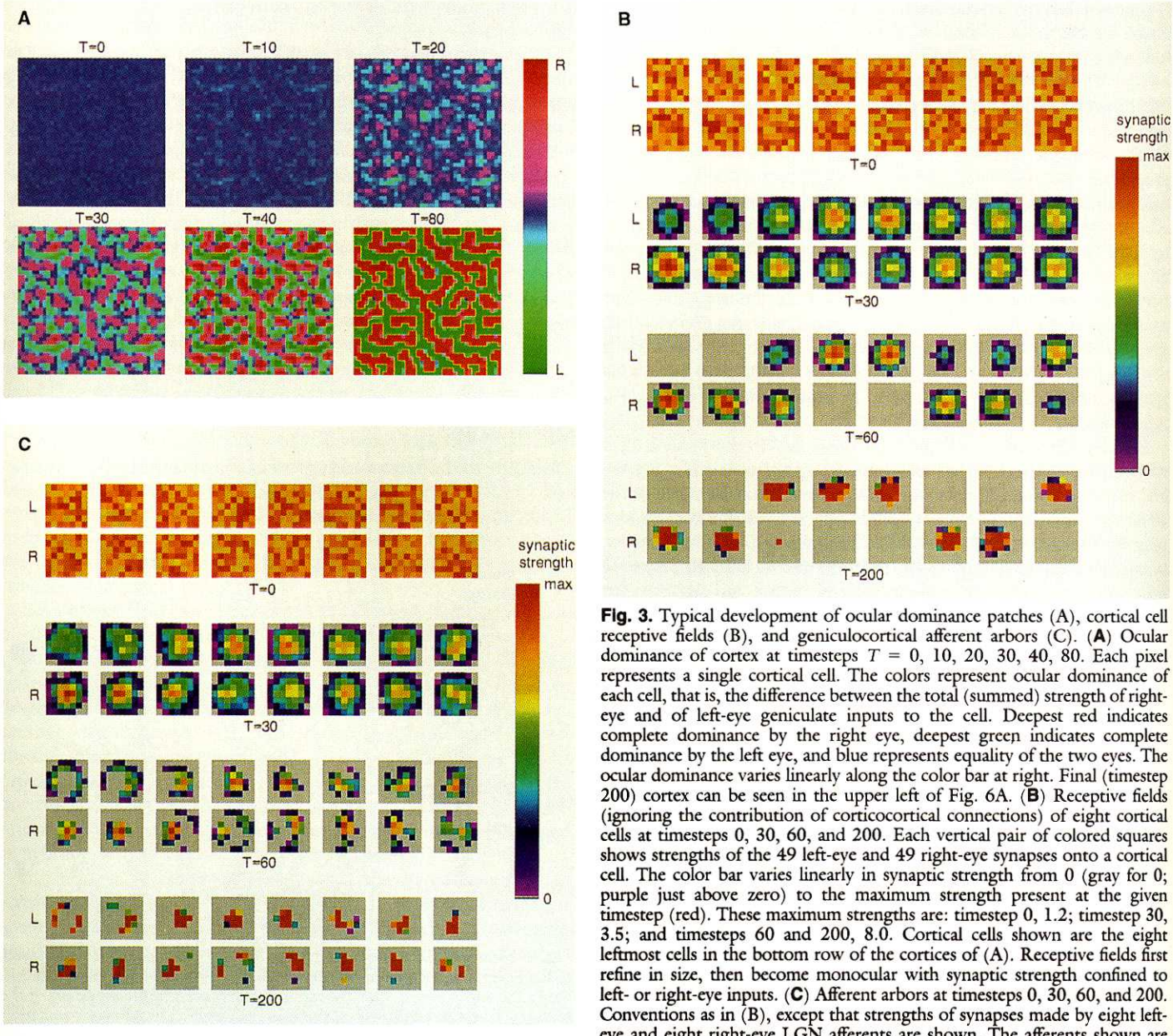

Fig. 3. Typical development of ocular dominance patches (A), cortical cell receptive fields (B), and geniculocortical afferent arbors (C). (**A**) Ocular dominance of cortex at timesteps T = 0, 10, 20, 30, 40, 80. Each pixel represents a single cortical cell. The colors represent ocular dominance of each cell, that is, the difference between the total (summed) strength of right-eye and of left-eye geniculate inputs to the cell. Deepest red indicates complete dominance by the right eye, deepest green indicates complete dominance by the left eye, and blue represents equality of the two eyes. The ocular dominance varies linearly along the color bar at right. Final (timestep 200) cortex can be seen in the upper left of Fig. 6A. (**B**) Receptive fields (ignoring the contribution of corticocortical connections) of eight cortical cells at timesteps 0, 30, 60, and 200. Each vertical pair of colored squares shows strengths of the 49 left-eye and 49 right-eye synapses onto a cortical cell. The color bar varies linearly in synaptic strength from 0 (gray for 0; purple just above zero) to the maximum strength present at the given timestep (red). These maximum strengths are: timestep 0, 1.2; timestep 30, 3.5; and timesteps 60 and 200, 8.0. Cortical cells shown are the eight leftmost cells in the bottom row of the cortices of (A). Receptive fields first refine in size, then become monocular with synaptic strength confined to left- or right-eye inputs. (**C**) Afferent arbors at timesteps 0, 30, 60, and 200. Conventions as in (B), except that strengths of synapses made by eight left-eye and eight right-eye LGN afferents are shown. The afferents shown are the eight leftmost cells in the bottom row of the geniculate grids. Note that arbors first refine, then break up into patches confined to complementary ocular dominance stripes. This development used the following functions: The correlation functions have same-eye correlations only, with Gaussian parameter 2.8 (Fig. 5A). The intracortical interactions are mixed excitatory-inhibitory (Fig. 5B). The arbor function is taken to be 1 over a 7 × 7 arbor, 0 elsewhere. Conventions for all simulations: Illustrations of cortex show 40 × 40 grids, although the model cortex is 25 × 25. Periodic boundary conditions were used, so this display shows continuity of the pattern across what would otherwise appear to be a boundary. Simulations in most cases were run through timestep (iteration) 200; the cortex was mature by timestep 60 to 100, and very few or no changes were visible in the cortical maps after timestep 150. For the range of functions considered in this article, all but 2,500 to 4,000 of the 61,250 synapses had limiting values of 8.0 or 0.0 at timestep 200.

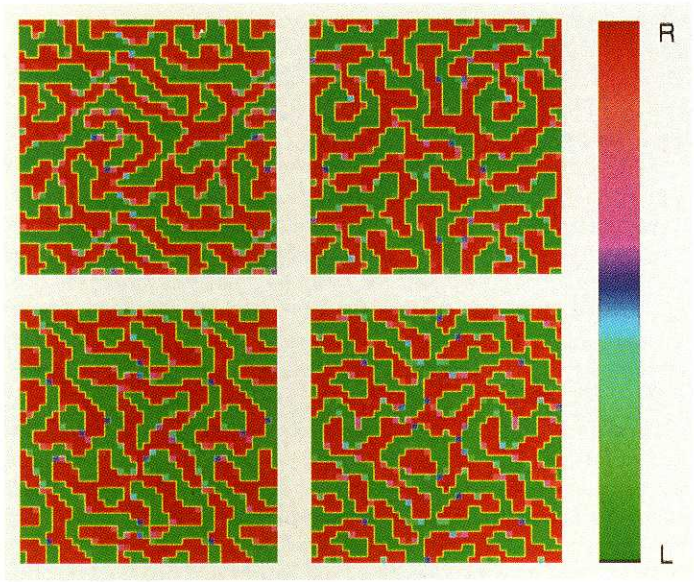

Fig. 4. Cortex, timestep 100, for four different random initial conditions. Cortical interaction, arbor, and correlation functions and conventions as in Fig. 3A. Results are qualititatively and quantitatively similar for all initial conditions we have tried; that is, the two-dimensional Fourier transforms yield similar power spectra.

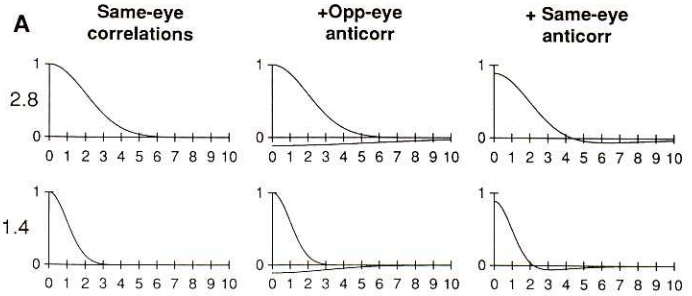

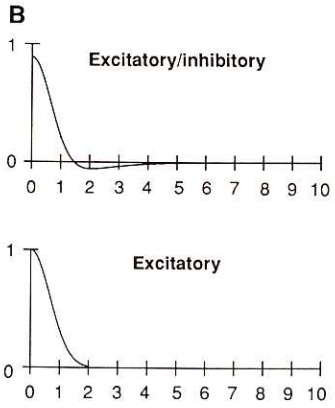

Fig. 5. Correlation functions (A) and cortical interaction functions (B) used in simulations and computations. Horizontal axes are in units of grid intervals. All functions are circularly symmetric in two dimensions. (**A**) Correlation functions. Functions labeled "same-eye correlations" represent positive correlations, as illustrated, between afferents within each eye, with zero correlation between the eyes. The functions illustrated are Gaussians e^{-x^2/ξ^2}, with parameters ξ = 2.8 and 1.4, respectively. Results do not depend on the Gaussian tails. Results with ξ = 2.8 are virtually identical if the function is set to zero outside a square of ±3 grid intervals, that is, outside an arbor radius. Results with ξ = 1.4 change only slightly if the function is set to zero outside a square of ±1 grid interval. Functions labeled "+opp-eye anticorr" include anticorrelations between afferents from the two different eyes, illustrated by the curve below the axis, in addition to the positive correlations within each eye as in the same-eye correlations case. Functions labeled "+same-eye anticorr" have anticorrelations added within each eye, in addition to the positive correlations within each eye, while correlations between the two eyes remain zero. Both opposite-eye and same-eye anticorrelations are given by the Gaussian $-(1/9)\, e^{-x^2/(3\xi)^2}$ with ξ the same as for the same-eye correlations. (**B**) Cortical interaction functions. The mixed "excitatory-inhibitory" function is given by $e^{-x^2/\xi^2} - (1/9)\, e^{-x^2/(3\xi)^2}$ with ξ = 0.933. It was explicitly set to zero outside a square of ±7 grid intervals. Results are identical if the cutoff is ±5 grid intervals, and only small changes are seen if the cutoff is ±3 grid intervals. The "excitatory" function consists of the excitatory Gaussian alone, explicitly set to zero outside a square of ±2 grid intervals. Results are indistinguishable with a cutoff of ±1 grid interval.

As Fig. 8 indicates, the characteristic receptive fields have associated with them characteristic afferent arbors, given by multiplying the receptive field by the oscillation in ocular dominance. In other words, when characteristic receptive fields are monocular, so that ocular dominance patches arise, the afferent arbors will only innervate the patches from the relevant eye. Thus, characteristic arbors show patches with a periodicity equal to that of the cortical oscillation, as is seen both in the simulations and in actual biological development.

Determining the Monocularity and Periodicity of Cortex

If the fastest growing characteristic receptive field is monocular, then a pattern of ocular dominance patches will form. The patch width is given by the wavelength of the fastest growing pattern. Thus, our problem can be reduced to two questions. (i) Under what circumstances will the fastest growing field be monocular? (ii) If it is monocular, what determines its wavelength?

Solution of the equation in simple limiting cases suggests that the correlation function C^D determines the wavelength of oscillations of ocular dominance across a receptive field, whereas the cortical interaction function I determines the wavelength of oscillations across an arbor. In these limits, each wavelength is given by the dominant wavelength in the corresponding function. This is the wavelength corresponding to the peak of that function's Fourier transform. The oscillation of ocular dominance across the cortex is the superposition of these two oscillations. Thus, if C^D does not oscillate within an arbor radius, the fastest growing receptive field does not oscillate and hence is monocular. The wavelength of the fastest growing pattern is then given by the dominant wavelength in I. Each limiting case leads to an analytic expression for the growth rate of each cortical wavelength of ocular dominance in terms of arbors, correlations, and cortical interactions (*12, 13*).

Direct computation of the characteristic patterns of ocular dominance for a variety of parameters confirms these basic results (*31*). Figure 9A shows the growth rates of characteristic patterns as a function of their wavelength, for the functions used in Fig. 6A. Gray level indicates the monocularity of the corresponding receptive fields, where lightest is fully monocular and darkest is fully binocular. The fastest growing field is monocular whenever $C^D(\alpha - \beta)$ is locally positive, that is, positive at least between nearest neighbors on a grid, and nonnegative within an arbor radius. Broader correlations or opposite-eye anticorrelations increase the monocularity of fields and the advantage in growth rate of monocular over binocular fields. Same-eye anticorrelations have the opposite effects. Their presence within an arbor radius (same-eye anticorr 1.4) leads binocular fields to grow fastest. In all cases, the wavelength of the fastest growing monocular pattern is determined by the peak of the Fourier transform of the cortical interaction function $I(x - y)$ (light lines in Fig. 9A) in close accordance with predictions from limiting cases (heavy lines in Fig. 9A).

There is an exception if the wavelength of a monocular pattern is much larger than an arbor diameter. Then in order for the pattern to grow, entire arbors centered within a dominance patch must either increase in strength or decrease in strength. If there is a constraint limiting the total synaptic strength supported by a single arbor, arbors will be constrained to break up, so that a gain in synaptic strength in one part of the arbor is offset by a loss in another part. Such a constraint can limit the patch width to approximately one

arbor diameter (*32*). Figure 9B shows the growth rates of patterns, in the presence and absence of these constraints, for the two intracortical interactions of Fig. 5B. The excitatory cortical interaction normally selects a long wavelength but selects a wavelength of about an arbor diameter in the presence of constraints. The excitatory-inhibitory cortical interaction normally selects a smaller wavelength, and development under this interaction is not affected by these constraints.

To summarize, suppose that the correlation functions are such that C^D is locally positive and nonnegative within an arbor radius, so that cells tend toward monocularity. Then the patch width is determined by the dominant wavelength in the cortical interaction function $I(x - y)$. If the dominant wavelength is no larger than an arbor diameter, the patch width is equal to this wavelength. If it is larger than an arbor diameter and the total afferent arbor synaptic strength is sufficiently constrained, then the patch width is equal to the arbor diameter. The wavelengths of cortical ocular dominance in simulations, as determined by the two-dimensional Fourier transform of the patterns, develop in accordance with these rules (*13*).

Many Biological Mechanisms Can Be Modeled in This Framework

The results we have presented are not unique to a Hebbian synapse mechanism. A variety of other correlation-based mechanisms can be expressed in terms of an effective arbor function, an afferent correlation function, and a cortical interaction function. Therefore, they can be studied within our mathematical framework, as we shall now show for simplified versions of three alternative mechanisms.

First, suppose that cortical cells release diffusible or actively transported substances in proportion to their activity. Suppose that these substances are taken up by synapses in proportion to synaptic activity, as would be expected if uptake occurs in conjunction with vesicle reuptake, and that they modify synaptic strength. Let $E(x - z)$ describe an effective concentration of the substance at cortical site x resulting from release of a unit amount of the substance at cortical site z. Then, if we assume a plasticity rule for individual synapses of the form $\Delta s = [(conc)(pre) - decay]\Delta t$, where *conc* is a linear function of the substance's concentration, and *pre* is again a function of presynaptic activity, we obtain Eq. 1. In this case the intracortical interaction $I(x - y) = \sum_z E(x - z)H(z - y)$, where $H(z - y)$ is the intracortical interaction of the Hebbian case arising from intracortical synaptic interactions (*33*).

Second, we suppose a plasticity rule as just described, except that afferents rather than cortical cells release the modification factor in proportion to the strength of their activity. This leads to Eq. 1, with the intracortical interaction $I(x - y) = E(x - y)$. In this case the activity of cortical cells has no influence on plasticity (*34*).

Third, suppose that in addition to modifiable synapses, we consider chemospecific adhesion between afferent and cortical cells. Such "retinotopic" adhesion has been considered important in many models of retinotectal connections (*19, 35*). Suppose the degree of chemospecific adhesion between the afferent from α and the cortical cell at x depends only on $x - \alpha$. In this case, the retinotopic adhesion can be represented by a factor $f(x - \alpha)$ multiplying some of the terms on the right side of Eq. 1. This is formally the role played by the arbor function. Hence, by letting $A(x - \alpha)$ represent the product of the chemospecific adhesion times the arbor strength, we can take account of retinotopic adhesion.

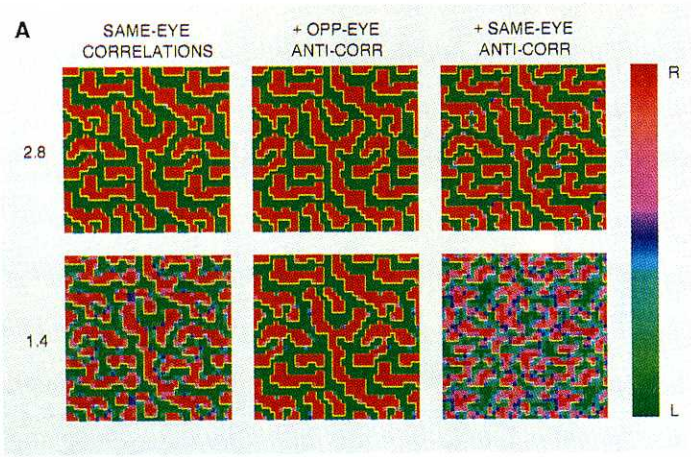

Fig. 6. Development of ocular dominance using different correlation (A) and cortical interaction (B) functions. Initial conditions, conventions, and all functions (correlation, cortical interaction, arbor) except the one being studied are as in Fig. 3A. (**A**) Cortex, timestep 200, resulting from development from timestep 0 with each of the six afferent correlation functions illustrated in Fig. 5A. (**B**) Cortex, timestep 200, resulting from development from timestep 0 with the purely excitatory cortical interaction function (Fig. 5B). For these simulations, constraints were used fixing the total synaptic strength over each afferent arbor. In (A), these constraints make little difference in the final results (for example, compare the lower right panel of Fig. 7, which used only partial constraints, with the upper right panel of Fig. 6A). In (B), results depend crucially on these constraints. The theoretical basis for this difference is discussed in the text and in Fig. 9B.

Discussion

We have formulated and analyzed a class of models of cortical ocular dominance development. They predict the development of a periodic pattern of ocular dominance like that seen experimentally. The organization of periodicity requires three conditions:

1) The correlation function $C^D = C^{LL} - C^{LR}$ must favor formation of monocular cells, by being positive locally and not significantly negative within an arbor radius.

2) There must be intracortical interactions, which should be locally excitatory (*36*).

3) If the intracortical interactions are purely excitatory, there must be constraints on the total synaptic strength over an arbor. Given these conditions, a patch width of left-eye plus right-eye ocular dominance patches is determined. It corresponds to the wavelength at which the Fourier transform of $I(x)$ is maximized, provided that wavelength is less than an arbor diameter. Otherwise, if arbor constraints exist, the patch width will be approximately an arbor diameter. These results are very robust, being independent of initial conditions, nonlinearities, and the detailed form of the three functions.

These results are consistent with the measured sizes of ocular dominance patches, correlations, cortical interactions, and arbors in the adult cat (*5–9*). The observed patch width of about 850 μm can be produced by a variety of intracortical interactions ranging from excitation over a radius of 50 μm or less surrounded by weak inhibition to excitation over 200 μm or more surrounded by strong

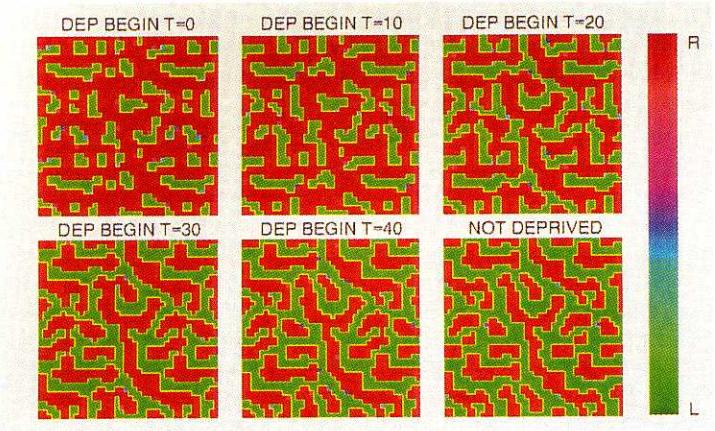

Fig. 7. Results of monocular deprivation. Results at timestep 200 are shown for initiation of monocular deprivation at five different times (timestep 0, 10, 20, 30, and 40). The sixth panel shows, for comparison, timestep 200 in an identical run but without deprivation. Arbor, correlation, and cortical interaction functions, initial conditions, and conventions as in Fig. 3A except as follows. Monocular deprivation is modeled as 30% decrease of amplitude of correlation function within deprived eye. Constraints on total synaptic strength over afferent arbors allow each arbor to decrease or increase its total synaptic strength by up to 50%. Without some constraint limiting changes in total synaptic strength over an arbor, one eye would completely take over cortex with early onset of deprivation. Although the choices of activity and constraint levels are arbitrary, the qualitative results are robust: with early onset of deprivation, the open eye takes over cortex to the limits imposed by constraints; with later onset, deprivation has progressively less effect.

inhibition. Periodic longer range corticocortical connections, if present in the young animal, could enhance the growth of patterns with a similar period. Alternatively, a variety of arbor sizes, ranging from flat arbors of diameter about 850 μm to larger tapering arbors, would yield 850-μm patch widths by an arbor-driven mechanism. Such a mechanism is consistent with X-cell, though not with Y-cell, initial arbor sizes.

Many other observed features of biological development emerge from the mechanisms studied. These include refinement of receptive fields and development of monocularity, refinement of arbors and their confinement to patches, monocular deprivation plasticity with a critical period, and an increase in monocularity resulting from treatments such as artificial strabismus or alternating monocular deprivation that reduce correlations or produce anticorrelations between activity in the two eyes.

Many of these developmental details are less robust than the development and organization of periodicity. The robust elements of these results involve relative rates of growth and depend on interactions between synapses. Periodicity develops because one eye's synapses grow faster than the other's within each ocular dominance patch. Similarly, central synapses in a receptive field grow faster than peripheral ones. The less robust elements of the results involve absolute rates of growth and depend on the range of total synaptic strength allowed for each synapse and for the summed synaptic strength over each cell. For example, when a periodic difference in the strengths of the two eyes develops, the synapses of the weaker eye in a patch may decrease in strength or they may simply grow more slowly than the dominant eye's synapses. Only in the former case will individual cells become monocular. This can occur if there is a constraint limiting the total synaptic strength over a cortical cell and if individual synapses can grow sufficiently so that a single eye's synapses can saturate a cortical cell. In the absence of such constraints, one may see periodicity in each eye's innervation without seeing organization of monocular patches. Such a result may be seen in some New World monkeys (*37*).

Limitations on the range of synaptic strengths can be achieved by many means (*16, 17, 19–22, 38*). Because little is known about the actual mechanisms involved biologically, we prefer to use simple mechanisms, which can be analyzed more easily, for modeling purposes (*39*).

Other Models

Some earlier models of ocular dominance (*3*) showed that patches could form from simple mechanisms like those studied here. Others (*20, 40*) focused on the development of monocularity in isolated cells, as well as on dynamical means of limiting synaptic strengths. Legendy (*18*) studied a Hebb-like model and concluded that intracortical synaptic interactions will determine the distances over which cortical cells are similar in their response properties.

Swindale (*41*) formulated a model in terms of an effective interaction across cortex between right-eye and left-eye synapses, which produced stripes like those obtained here. The precise nature of this interaction was not specified. In the limit in which the correlation function C^D is constant or slowly varying, the influence of one synapse on another depends only on their cortical locations and their eyes of origin, and not on their retinotopic locations. Then the present model can be reduced mathematically to Swindale's (*12, 13*). We can then express his effective interaction in terms of arbors, cortical interactions, and afferent correlations.

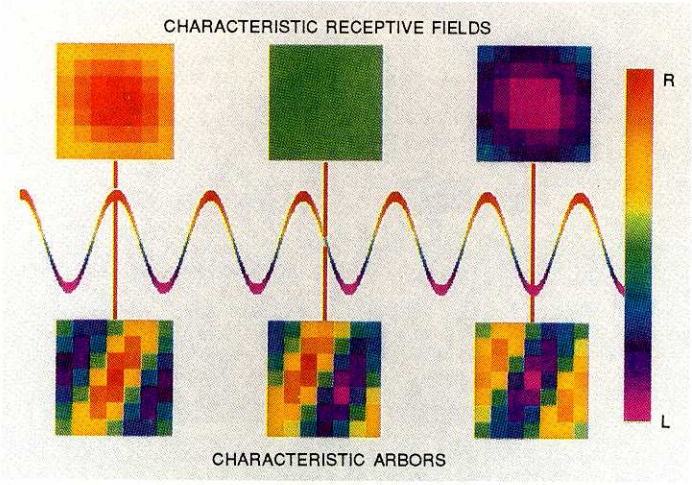

Fig. 8. Illustration of typical monocular characteristic pattern of ocular dominance. The characteristic receptive field, and associated characteristic arbor, at three cortical points are illustrated. The sinusoid indicates the oscillation of ocular dominance across cortex associated with a characteristic pattern. Color codes S^D, the difference between the synaptic strengths of the two eyes, varying from dominance by one eye to dominance by the other. At the cortical point corresponding to the leftmost receptive field, cortical cell inputs are dominated by the right eye. Afferents with the corresponding retinotopic position therefore project arbors such that the right eye afferents preferentially project to the central patch of the arbor (cortical right-eye stripe) and the left-eye afferents preferentially project to the peripheral patches (left-eye cortical stripe). Similarly, the central receptive field is at the border between left-eye and right-eye stripes, where the two eyes have equal innervation, and the rightmost receptive field is in the center of a left-eye stripe. The pattern shown here is one of the set (identical except for rotations of the direction of the oscillation) of fastest growing characteristic patterns for the functions used in Fig. 3. The oscillation is shown correctly scaled to the arbor and receptive field sizes. The oscillation projects in a direction perpendicular to the stripes across the arbors rather than horizontally as depicted.

Linsker (*21*) developed a model of plasticity very much like ours, which he used to study the development of orientation selectivity in visual cortex. It differs from ours in allowing modifiable input synapses to be excitatory or inhibitory, in using Gaussian arbors, in using constraints that ultimately fix the summed excitatory and the summed inhibitory input to a cortical cell, and in studying input from only a single eye. Our eigenfunction analysis can provide insight into his results. Thus, our equation for S^D can alternatively be regarded as an equation for the strength of synapses, of one eye, that can be positive or negative. "Center-surround" cells develop in his model, because the fastest growing eigenfunctions have receptive fields that concentrate their strength centrally. When combined with constraints that force 35% of final synapses to be negative (*42*), this can lead to a center of positive synapses with a surround of negative synapses. Therefore, the development of "center-surround" cells and the corresponding development of anticorrelations in the afferent correlation function depend on the negative synapses and the constraints. Given an afferent correlation function with strong anticorrelations within an arbor radius, oriented cells can develop. This is related to the fact that the fastest growing eigenfunctions for such a case (same-eye anticorr 1.4) have receptive fields that are striped.

Pearson, Finkel, and Edelman (*43*) developed a similar, but more complex, model to study somatosensory development and plasticity. By examining this model in terms of arbors, correlations, and cortical interactions, we conclude that the periodicity that develops in it should scale with the cortical interactions. If these interactions extend over several hundred micrometers, the "groups" found in that model also extend over several hundred micrometers. Physiologically, no such structures exist on such a large scale (*44*). Hence, our analysis would rule out their model without significant modification.

These points will be discussed elsewhere at greater length (*13, 14, 45*).

Experimental Implications

Our model can serve as a guide for experiment. We have found that local correlations over an arbor radius determine the development of monocularity, whereas cortical interactions determine the width of ocular dominance patches up to a possible limit set by arbor diameters. Measurement of initial correlation, cortical interaction, and arbor functions in various brain regions or species can test whether a proposed developmental mechanism is consistent with the patch width that emerges in each case. For example, area 18 of the cat has patches 1.5 to 2 times wider than those in area 17; arbors, and perhaps correlations, are also more widespread (*5, 6, 46*). If a Hebbian mechanism is responsible, we predict that kittens will show either a difference between the two regions in intracortical connectivities sufficient to account for the difference in patch width or predominantly excitatory intracortical connections in both regions resulting in arbor-limited patch widths.

Perturbation of the three functions in an experimental preparation before the onset of segregation, and comparison of the resulting patch width to the unperturbed case, can also test mechanisms.

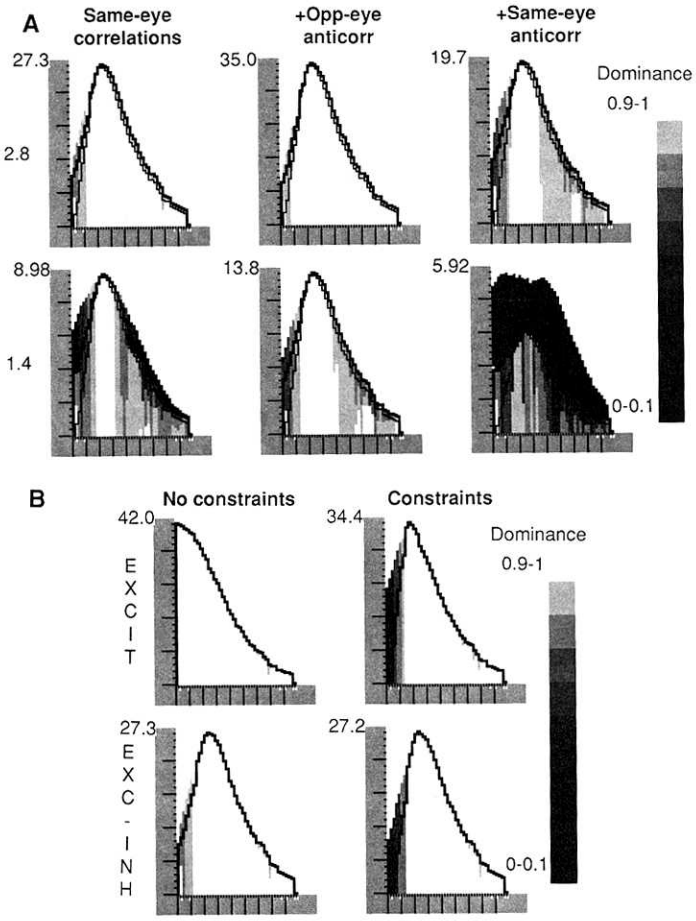

Fig. 9. Computed growth rate (vertical axes) of characteristic patterns of ocular dominance, as a function of inverse wavelength of the pattern (horizontal axes), for varying choice of (A) correlation and (B) cortical interaction functions. Grayscale indicates maximum dominance of any characteristic pattern with the given wave number and growth rate. Dominance is a measure of the degree of monocularity of the pattern's characteristic receptive field, on a scale from 0 for complete binocularity to 1 for perfect monocularity. Number beside the vertical axis indicates the maximum growth rate of any pattern. The horizontal axis represents wave number; the wavelength in units of grid intervals is 25 divided by the wave number. The first bin on the horizontal axis represents wave numbers 0 to 0.23; subsequent bins represent increments of 0.4 in wave number, so that the second bin represents wave numbers 0.23 to 0.63, and so forth. Bins representing wave numbers for which there can be no characteristic pattern, because of the nature of our grid, are indicated with a white mark on the horizontal axis; for each dominance, these bins are assigned a growth rate that is the average of that of the two adjoining bins. (**A**) The six correlation functions of Fig. 5A. Arbor and cortical interaction functions are as in Fig. 3; there are no constraints on total synaptic strength over an arbor. The heavy lines show an analytic prediction for growth rate of each cortical wavelength of ocular dominance in terms of the cortical interaction and arbor functions and the correlation functions in each case. This prediction is normalized to the maximum growth rate of characteristic patterns with dominance ≥ 0.5. The light lines show the Fourier transform of the cortical interaction function, identically normalized. We derived the analytic expression by assuming that correlations change slowly over an arbor diameter. However, it accurately predicts the growth of monocular patterns over a wide range of correlation functions. At its peak, which is the dominant wavelength in the cortical interaction, the degree of monocularity and the growth rate of monocular patterns are enhanced. (**B**) The two cortical interaction functions of Fig. 5B. Arbor and correlation functions as in Fig. 3. Two cases are shown: with constraints that fix the total synaptic strength over each afferent arbor and without any constraints on that total synaptic strength. Black lines indicate predictions of the analytic expression obtained as described in (A). The constraints suppress the growth of monocular patterns with wavelength longer than an arbor diameter. Constraints have a profound effect on the outcome when the excitatory cortical interaction function is used. They select a wavelength of an arbor diameter: the maximum growth rate in the figure for this case occurs at wavelengths of 7.3 to 8.3 grid intervals. Constraints have little effect on the outcome when the mixed excitatory-inhibitory interaction function is used. This function normally selects a wavelength shorter than an arbor diameter. In this case, the maximum growth rate occurs at wavelengths of 5.4 to 5.9 grid intervals.

Under the hypothesis that a Hebbian mechanism underlies ocular dominance plasticity, periodic segregation is driven by intracortical synaptic connections. Local infusion of muscimol, a γ-aminobutyric acid (GABA) agonist, which inhibits postsynaptic cells, will eliminate activation of such connections. Therefore, we would predict that no pattern of ocular dominance organization would be seen in the muscimol-infused region, although individual cells might become monocular. Alternatively, intracortical inhibitory connections may be blocked by local infusion of bicuculline, a GABA antagonist. An increase in patch width would be consistent with a Hebbian mechanism, with width determined by the intracortical interactions. If patch width were unchanged by bicuculline, one would conclude either that the period was normally arbor-limited (which could be tested by measuring whether intracortical interactions were predominantly excitatory during initial column development) or that a non-Hebbian mechanism was involved.

The model predicts that broader correlations within each eye would increase monocularity of layer 4 for mechanisms of the type we study. This could be tested by inducing broader correlations through pharmacological interventions in the retinas. One could also measure whether retinal correlations are broadened in animals deprived of pattern vision. Such animals have increased numbers of monocular cortical neurons (*47*). It would also be of interest to determine whether geniculate correlations are broader, relative to a geniculocortical arbor radius, in the developing monkey than in the kitten, because the monkey develops a more fully monocular layer 4 (*24, 26*).

Conclusion

A variety of biological mechanisms will robustly cause development of a periodic structure of ocular dominance. The patch width can be predicted from a few biological functions that are, in principle, measurable. Given biologically plausible conditions to limit the synaptic strengths, these mechanisms also result in refinement and development of monocularity in individual receptive fields, the confinement of arbors to patches, and monocular deprivation plasticity including a critical period. These results lend plausibility to the notion that simple mechanisms of activity-dependent competition may underlie many of the phenomena seen in the developing visual nervous system.

REFERENCES AND NOTES

1. T. N. Wiesel and D. H. Hubel, *J. Neurophysiol.* **28**, 1029 (1965); R. W. Guillery, *J. Comp. Neurol.* **144**, 117 (1972). For a review of the material summarized in this paragraph, see M. P. Stryker, in *The Biology of Change in Otolaryngology*, R. J. Ruben, T. R. Van De Water, E. W. Rubel, Eds. (Elsevier Science, Amsterdam, 1986), pp. 211–224.
2. G. S. Stent, *Proc. Natl. Acad. Sci. U.S.A.* **70**, 997 (1973); J.-P. Changeux and A. Danchin, *Nature* **264**, 705 (1976); H. Wigstrom and B. Gustafsson, *Acta Physiol. Scand.* **123**, 519 (1985).
3. C. von der Malsburg and D. J. Willshaw, *Exp. Brain Res. Suppl.* **1**, 463 (1976); C. von der Malsburg, *Biol. Cybern.* **32**, 49 (1979).
4. Some of these results have appeared previously in abstracts: K. D. Miller, J. B. Keller, M. P. Stryker, *Soc. Neurosci. Abstr.* **12**, 1373 (1986); K. D. Miller and M. P. Stryker, *ibid.* **14**, 1122 (1988); K. D. Miller, J. B. Keller, M. P. Stryker, *Neural Networks* **1**, S266 (1988); K. D. Miller, M. P. Stryker, J. B. Keller, *ibid.*, p. S267.
5. C. J. Shatz, S. Lindstrom, T. N. Wiesel, *Brain Res.* **131**, 103 (1977); S. Lowel and W. Singer, *Exp. Brain Res.* **68**, 661 (1987); N. V. Swindale, *J. Comp. Neurol.* **267**, 472 (1988).
6. P. A. Anderson, J. Olavarria, R. C. Van Sluyters, *J. Neurosci.* **8**, 2183 (1988).
7. Putative Y-cell geniculocortical axon: S. LeVay and M. P. Stryker, *Soc. Neurosci. Symp.* **4**, 83 (1979). X-cell arbors have not been filled in the kitten; based on fills in adults, X cells may have initial arborizations 1 to 1.5 mm in diameter [A. L. Humphrey, M. Sur, D. J. Uhlrich, S. M. Sherman, *J. Comp. Neurol.* **233**, 159 (1985)].
8. Correlations in spontaneous firing, enduring over times of 1 to 10 ms in uniform light and about 50 ms in the dark, have been measured between retinal ganglion cells of adult cats [D. N. Mastronarde, *J. Neurophysiol.* **49**, 303 (1983); *ibid.*, p. 325]. The degree of correlation of two cells depends on the separation of their receptive field centers, which we may express as a distance across cortex [R. J. Tusa, L. A. Palmer, A. C. Rosenquist, *J. Comp. Neurol.* **177**, 213 (1978)]. Among cells of the same center type (on-cells or off-cells), X cells are correlated over distances representing about 350 μm across cortex, Y cells over about 1.6 mm; X cells are correlated with Y cells over about 1 mm. Cells of opposite center type are anticorrelated over similar distances. Fluctuations in spontaneous discharge of retinal and geniculate cells in adult cats in darkness over longer time scales (30 s to 30 min) appear to be synchronized throughout each eye but unsynchronized between eyes [R. W. Rodieck and P. S. Smith, *J. Neurophysiol.* **29**, 942 (1966); W. R. Levick and W. O. Williams, *J. Physiol. (London)* **170**, 582 (1964)].
9. R. Hess, K. Negishi, O. Creutzfeldt, *Exp. Brain Res.* **22**, 415 (1975); K. Toyama, M. Kimura, K. Tanaka, *J. Neurophysiol.* **46**, 191 (1981); C. D. Gilbert and T. N. Wiesel, *J. Neurosci.* **3**, 1116 (1983); H. J. Luhmann, L. Martinez Milan, W. Singer, *Exp. Brain Res.* **63**, 443 (1986); Y. Hata, T. Tsumoto, H. Sato, K. Hagihara, H. Tamura, *Nature* **335**, 815 (1988).
10. The quantities α and x are two-dimensional indices, for example, $\alpha = (\alpha_1, \alpha_2)$. They represent retinotopic positions in the LGN and cortex, respectively. To each α in the LGN there is a retinotopically corresponding $x(\alpha)$ in the cortex. We use $x - \alpha$ to mean $x - x(\alpha)$. Cells in the visual cortex are generated early (unlike retinotectal development) so that cortical growth need not alter retinotopy.
11. D. O. Hebb, *The Organization of Behavior* (Wiley, New York, 1949). *N*-methyl-D-aspartate (NMDA) receptors may provide a biological mechanism for Hebbian plasticity. See G. L. Collingridge and T. V. P. Bliss, *Trends Neurosci.* **10**, 288 (1987).
12. K. D. Miller and J. B. Keller, in preparation.
13. K. D. Miller and M. P. Stryker, in *Connectionist Modeling and Brain Function: The Developing Interface*, S. J. Hanson and C. R. Olson, Eds. (MIT Press/Bradford, Cambridge, MA, in press).
14. K. D. Miller, in *Neuroscience and Connectionist Theory*, M. A. Gluck and D. E. Rumelhart, Eds. (Erlbaum, Hillsboro, NJ, in press).
15. Let $c(x,t)$ represent activity (firing rate or membrane potential) of the cortical cell at location x at time t. Similarly, let $a^L(\alpha,t)$, $a^R(\alpha,t)$ represent firing rates of afferents serving the left or right eye, respectively, from locations α at time t. The equation used to describe Hebbian synapses is

$$\frac{dS^L(x,\alpha,t)}{dt} = \lambda A(x-\alpha)[c(x,t) - c_1]f_1[a^L(\alpha,t)] - \gamma S^L(x,\alpha,t) - \varepsilon' A(x-\alpha) \quad (3)$$

Let the geniculate input to y at time t be $G(y,t) = \sum_\alpha \{S^L(y,\alpha,t) f_2[a^L(\alpha,t)] + S^R(y,\alpha,t) f_2[a^R(\alpha,t)]\}$. The equation used to describe cortical activation is $c(x,t) = \sum_y I(x-y)G(y,t) + c_2$. In these equations, λ, γ, ε', c_1 and c_2 are constants; f_1 and f_2 are functions incorporating threshold and saturation effects. If $c(x,t) = G(x,t) + \sum_y B(x-y)c(y,t) + c'$, where **B** summarizes corticocortical interconnections, then the matrix $\mathbf{I} = (\mathbf{1} - \mathbf{B})^{-1}$.

We substitute the expression for $c(x,t)$ into Eq. 3, average the resulting equation over afferent activity patterns, and ignore higher order terms. Then we obtain Eq. 1, with $C^{LL}(\alpha - \beta) \equiv \langle f_1[a^L(\alpha,t)]\, f_2[a^L(\beta,t)]\rangle$, $C^{LR}(\alpha - \beta) \equiv \langle f_1[a^L(\alpha,t)]\, f_2[a^R(\beta,t)]\rangle$, and $\varepsilon \equiv \varepsilon' - \lambda(c_2 - c_1)\langle f_1[a^L(\alpha,t)]\rangle$, where pointed brackets indicate average value. We have kept the notation S for $\langle S\rangle$.

This model includes only a single type of afferent. Corticocortical connectivity is considered to be uniform and unchanging. Changes in geniculocortical synaptic strengths are assumed to produce the initial pattern of ocular dominance, so that sprouting or retraction of terminal branches is not considered. These changes are governed by activity correlations over a time scale determined by the plasticity mechanism [G. G. Blasdel and J. D. Pettigrew, *J. Neurophysiol.* **42**, 1692 (1979); L. Altmann, H. J. Luhmann, J. M. Greuel, W. Singer, *ibid.* **58**, 965 (1987); B. Gustaffsson, H. Wigstrom, A. C. Abraham, Y. Y. Huang, *J. Neurosci.* **7**, 774 (1987)]. Interactions on this or finer time scales are considered instantaneous. Rationales for simplifications are discussed in (*13, 14*).
16. D. J. Willshaw and C. von der Malsburg, *Proc. R. Soc. London Ser. B* **194**, 431 (1976).
17. S. Grossberg, *Biol. Cybern.* **21**, 145 (1976).
18. C. R. Legendy, *Brain Res.* **158**, 89 (1978).
19. V. A. Whitelaw and J. D. Cowan, *J. Neurosci.* **1**, 1369 (1981).
20. E. L. Bienenstock, L. N. Cooper, P. W. Munro, *ibid.* **2**, 32 (1982).
21. R. Linsker, *Proc. Natl. Acad. Sci. U.S.A.* **83**, 7508 (1986); *ibid.*, p. 8390; *ibid.*, p. 8779.
22. C. von der Malsburg, *Kybernetik* **14**, 85 (1973). We implement conservation of total synaptic strength over a cortical cell by subtraction of the same time-dependent quantity from each synapse on a cell, whereas von der Malsburg subtracted a time-dependent quantity times the synapse's strength. The latter method suppresses the development of ocular dominance unless opposite-eye anticorrelations are present. This is discussed in (*14*) and in K. D. Miller and D. J. C. MacKay, in preparation.
23. At each timestep, synapses are updated as follows: (i) Compute derivative (change per timestep) of each synapse from Eq. 1. $\gamma = \varepsilon = 0$. λ is set, for each choice of functions A, I, and C, so that the average change in S^D per timestep should initially be about 0.003. This yields $0.003 < \lambda < 0.015$. (ii) Modify derivatives with constraints. Constraints subtract a constant, weighted by $A(x-\alpha)$, from the derivative of each synapse $S^L(x-\alpha)$ or $S^R(x-\alpha)$ associated with a cell. The constant is determined for each cell so that the sum of derivatives over that cell becomes zero. First all cortical cells, and then all afferents, are constrained. (iii) Use these derivatives plus derivatives from previous timesteps to compute total change in each synapse by a three-step method [G. Birkhoff and G. Rota, *Ordinary Differential Equations* (Wiley, New York, 1978), p. 221], and update synaptic strengths. (iv) If $S^L(x,\alpha,t) < 0$ or $> 8A(x-\alpha)$, cut off value at 0 or $8A(x-\alpha)$,

respectively; similarly for S^R. (v) If any synapses have been cut off, correct the normalization of cortical cells. Each synaptic strength on the cortical cell at x is multiplied by a constant that sets total synaptic strength on the cell to $2\sum_{\beta} A(x - \beta)$.

In simulations of Fig. 7, only partial constraints on afferent arbors were used. The term subtracted from the derivative of $S^L(x,\alpha)$ was multiplied by

$$\text{minimum}\left[1.0, \left(1 - \frac{\sum_z S^L(z,\alpha)}{\sum_z A(z-\alpha)}\right)^2 \Big/ (0.5)^2\right]$$

and similarly for $S^R(x,\alpha)$. This allows total synaptic strength over each arbor to vary between 0.5 and 1.5 times its original value.

Runs illustrated used stabilization: when synapses reached $8A(x - \alpha)$ or 0, they were frozen so that no further changes in their strengths were allowed. Stabilization has no effect on final results, with one exception involving some cases of late onset of monocular deprivation, discussed in the text. To implement stabilization, frozen synapses were assigned a derivative of 0, and steps (ii) and (v) were applied only to unfrozen synapses. The multiplicative constants of step (v) were restricted to remain between 0.8 and 1.2.

24. D. H. Hubel, T. N. Wiesel, S. LeVay, *Philos. Trans. R. Soc. London Ser. B* **278**, 377 (1977).
25. C. D. Gilbert, *J. Physiol. (London)* **268**, 391 (1977).
26. C. J. Shatz and M. P. Stryker, *ibid.* **281**, 267 (1978).
27. D. H. Hubel and T. N. Wiesel, *J. Neurophysiol.* **28**, 1041 (1965); P. O. Bishop, G. H. Henry, C. J. Smith, *J. Physiol. (London)* **216**, 39 (1971).
28. H. O. Reiter and M. P. Stryker, *Proc. Natl. Acad. Sci. U.S.A.* **85**, 3623 (1988).
29. The linear analysis determines the initial development of a periodic pattern. The fastest growing patterns dominate exponentially, so their period determines the width of the patches. The form of the pattern of patches (for example, stripes versus patches versus hexagons, or long parallel stripes versus shorter branching stripes) is determined by nonlinear interactions between these fastest growing patterns and so is not addressed by our analysis. It is possible for such an initial pattern to be only metastable, so that eventually it may reorganize into a pattern with a different period determined by nonlinearities. This is unlikely in the ocular dominance system, as studies of development of ocular dominance columns [S. LeVay, M. P. Stryker, C. J. Shatz, *J. Comp. Neurol.* **179**, 223 (1978)] show no obvious change in periodicity between its earliest detection and the final adult pattern. With the use of voltage-sensitive dyes [G. G. Blasdel and G. Salama, *Nature* **321**, 579 (1986)], it may be possible to test this by following development of the columns within a single animal. Derivation of Eq. 2 using nonlinear functions for *post* in Eq. 3 and for cortical activation is discussed in (*13*).
30. Let $r \equiv x - \alpha$ and transform variables from (x,α) to (x,r). Then the right side of Eq. 2 becomes a simple convolution in the variable x. By Fourier transform in x the eigenfunctions must be of the form $e^{ik\cdot x}R_{k\xi}(r)$, where k is a pair of rational numbers and serves as one index for the eigenfunctions, and ξ is an additional index enumerating the receptive field modes for a given k. $e^{ik\cdot x}$ represents a cortical oscillation with wavelength $2\pi/|k|$. $R_{k\xi}(r)$ is a (complex) characteristic receptive field, because it represents the variation of the eigenfunction as r varies while cortical location x is fixed. The eigenfunctions can also be written $e^{ik\cdot\alpha}B_{k\xi}(r)$, where $B_{k\xi}(r) = e^{ik\cdot r}R_{k\xi}(r)$. B is a characteristic arbor, as it represents the variation of the eigenfunction as r varies while afferent location α is fixed.

If $I(x) = I(-x)$ and $C^D(\alpha) = C^D(-\alpha)$, the real part and imaginary part of a complex eigenfunction are both real eigenfunctions, with the same eigenvalue. These real eigenfunctions can be chosen of the form $\cos k\cdot x\, R^+(r) + \sin k\cdot x\, R^0(r)$, where R^0 has zero net ocular dominance ($\sum_r R(r) = 0$) and R^+ may have net ocular dominance (*12, 13*). If, as for the eigenfunction of Fig. 8, $R^0 \equiv 0$, then the eigenfunction is precisely of the simpler form discussed in the text.
31. Eigenfunctions were computed by applying Eq. 2 to 25 × 25 grids with 7 × 7 uniform arbors as in the simulations. An eigenvalue equation was obtained for $R_k(r)$ for each of the 625 cortical wave numbers k. By symmetry, only 91 of these equations are distinct. We diagonalize the resulting 49 × 49 complex matrix for each distinct k, using routines from the International Mathematical and Statistical Libraries.
32. More specifically, the constraint on arbors suppresses the growth of monocular modes with long enough wavelength to contribute significantly to the Fourier transform of the arbor function. One can also consider the effect of a constraint on the total synaptic strength supported by a cortical cell. Such a constraint can be imposed directly on the equation determining $S^S \equiv S^L + S^R$ and need not affect the equation determining S^D; hence, such a constraint can be imposed without influence on the development of periodicity.
33. Equation 3 is altered by substitution of $\sum_y E(x - y)c(y,t)$ for $c(x,t)$.
34. Equation 3 is altered by substitution of $\sum_y E(x - y)G(y,t)$ for $c(x,t)$, where $G(y,t)$ is defined in (*15*). This mechanism could not account for the results of pharmacological inhibition of visual cortical cells during monocular deprivation (*28*) and hence can be ruled out in visual cortex. However, formation of periodic patches is also seen in many other locations in the nervous system.
35. S. E. Fraser, *Dev. Biol.* **79**, 453 (1980).
36. This condition allows a positive peak in the Fourier transform of $I(x)$. This may also be achieved by other forms of $I(x)$, for example, a purely inhibitory $I(x)$ with fairly sharp edges. We have not explored whether such an $I(x)$ could produce patches robustly.
37. Reviewed by S. LeVay and S. B. Nelson, in *The Electrophysiology of Vision*, A. Leventhal, Ed. (Macmillan, London, in press).
38. T. J. Sejnowski, *J. Theor. Biol.* **69**, 385 (1977); E. Oja, *J. Math. Biol.* **15**, 267 (1982).
39. See discussion of realistic versus simplifying brain models in T. J. Sejnowski, C. Koch, P. S. Churchland, *Science* **241**, 1299 (1988).
40. M. F. Bear, L. N. Cooper, F. F. Ebner, *ibid.* **237**, 42 (1987).
41. N. V. Swindale, *Proc. R. Soc. London Ser. B* **208**, 243 (1980).
42. This is the case when Linsker's parameter $g = 0.15$ (*21*).
43. J. C. Pearson, L. H. Finkel, G. M. Edelman, *J. Neurosci.* **7**, 4209 (1987).
44. M. M. Merzenich *et al.*, *J. Comp. Neurol.* **258**, 281 (1987).
45. D. J. C. MacKay and K. D. Miller, in preparation.
46. A. L. Humphrey, M. Sur, D. J. Uhlrich, S. M. Sherman, *ibid.* **233**, 190 (1985).
47. Reviewed in S. M. Sherman and P. D. Spear, *Physiol. Rev.* **62**, 738 (1982).

48. We thank R. Durbin and C. J. Shatz for helpful comments on the manuscript. Supported by a National Science Foundation (NSF) predoctoral fellowship to K.D.M. and by grants from the McKnight and System Development Foundations to M.P.S. Simulations were done at the San Diego Supercomputer Center supported by the NSF.